e-ISSN: 2548-060X

International Journal of Energy Applications and Technologies

journal homepage: www.dergipark.gov.tr/ijeat

Original Research Article

Study on the modeling and simulation of a grid-connected battery energy storage system based on cascaded h-bridge converter

Yousif Mustafa Sadeq Al-khdhairi, Ahmet Mete Vural*

Electrical and Electronics Engineering Department, Engineering Faculty, Gaziantep University, 27310-Şehitkamil/Gaziantep, Turkey

ARTICLE INFO

* Corresponding author
mvural@gantep.edu.tr

Received May 24, 2021
Accepted September 7, 2021

Published by Editorial Board Members of IJEAT

doi: 10.31593/ijeat.941900

ABSTRACT

Battery energy storage system (BESS) is evolving to be a major part of the modern power systems due to high controllability and simple implementation. In this paper, the general structure of the BESS and its components are reviewed focusing mainly on the battery storage unit in hierarchal order from cell to pack in terms of modeling, design, and wiring. The effect of the weakest cell and cell-to-cell variations are also mentioned in perspective of the battery charging and their effects on the wiring topology. Moreover, cascaded h-bridge (CHB) converter topology is also discussed and compared with other power electronic interfaces in terms of storage capacity and switching elements. It is shown that CHB converter topology can be utilized in BESS to minimize the number of series connected batteries. Finally, a 1 MWh 34.5 kV grid-connected BESS based on CHB converter topology is designed and simulated to test the capabilities of the BESS to supply active power to the power grid under closed-loop control.

Keywords: Battery energy storage system; Li-ion battery; Cascaded H-bridge converter; DC-DC converter

1. Introduction

The continuous expansion of the power systems around the globe cause a major impact on both the environment due to the increase in burning fossil fuels which is main source of carbon dioxide emission, and the power system stability that struggles to keep up with that growth to maintain balance between the generation and demand of electrical energy. Even though the integration of renewable energy source (RES) such as wind and solar energies has increased over the last decades to fill as a greener alternative energy resources, it suffers from low-density and intermittent generation that could harmfully affect the stability of the power systems [1-3]. The battery energy storage system (BESS) can be considered as a viable solution for these issues due to its high energy density, high efficiency, and fast control response. A BESS uses many batteries as the storage device to store excess energy from different sources and discharge them during time of high demand or congestion. Thereby, The BESS can be applied for diverse kinds of applications in different scales and fields in power systems. A BESS can be used in transportation sector to power up electric vehicles and their charging stations, or a BESS can be integrated with a RES to smooth the output power and compensate for the intermittent power generation, or a BESS can also be implemented in grid-scale applications to provide different types of ancillary services to the distribution and transmission networks such as power quality services (e.g. frequency and voltage regulation, and etc.) and energy applications (e.g. load leveling, peak shaving, energy arbitrage, and etc.) [4-5]. There are various types of secondary rechargeable batteries that are used in BESS such as lead-acid, Li-ion, and sodium sulphur batteries. Each battery type has its own chemistry, charging/discharging characteristics, and energy/power density levels. Due to the consistent demand on Li-ion batteries for the highest

efficiency and specific energy, their prices are on continuous decline which make them feasible for all kinds of applications from electrical vehicle to stationary grid scale BESS. Generally, the nominal voltage of Li-ion batteries lies in the range between 3.0 and 4.2V depending on the battery chemistry. Therefore, in order to construct a BESS in grid scale of megawatts capacity connected to medium voltage level distribution networks, multiple batteries have to be connected in series to meet the voltage requirements. Also, several batteries have to be connected in parallel to reach the desired energy storage capacity. However, piling up more batteries in series/parallel connections for grid scale could cause a decline in the BESS reliability and imbalance between the state of charge (SOC) of the battery cells that lead to a downfall in the battery lifetime can occur [6]. Thus, different design approaches are proposed in the literature to find more reliable and efficient ways to install BESS for large-scale grid applications to provide higher voltage and power capacity by considering modular design and power electronic interfaces. In [7-8], the series/parallel connected battery modules are interfaced with a dc-dc and ac-dc converter to obtain higher voltage levels with high reliability. In [9], a new modular reconfigurable battery pack is introduced which is comprised of single or several cascaded reconfigurable battery modules connected to a H-bridge converter. Each battery pack needs only one power electronic switch to charge and discharge the battery cells. Such a design allows better control over the battery cells and disconnects only the faulty cell without disrupting the BESS operation. Consequently, this design features fault-tolerance and high-reliability with least power switch requirements. A review on different kinds of reconfigurable battery techniques and designs is presented in [10]. In [11], the integration of modular multi-level converter (MMC) for a BESS is considered. In [12-13], a real large-scale BESS rated at 10kV and 2MW in Shenzhen city of China is suggested which is based on cascaded h-bridge (CHB) converter topology. The CHB comprises of cascaded connected power modules that consist of the energy storage device, dc-link capacitor, and H-bridge converter. In [14], a comparison simulation study is performed between CHB and MMC topologies for BESS integration. The study shows that CHB topology outperforms MMC for BESS usage in terms of efficiency and lower count of switching devices. In [15], three different designs such as power block design, intelligent battery pack, and CHB topology are considered for large-scale BESS application rated at 11 kV and 1MWh. Three approaches are evaluated in terms of cell losses and the power electronic devices based on Markov-based modeling. It is found that intelligent battery pack and CHB designs are more favorable due to their fault-tolerant and build-in SOC capabilities. This study gives detailed information on the modeling and simulation of a grid-connected battery energy storage system based on cascaded h-bridge converter. After the introduction section, typical BESS components are reviewed in Section 2.

Section 3 presents the details of the BESS control scheme including decoupled current control scheme and the dc link voltage controller. The simulation results of a 1MWh BESS connected to a 34.5 kV distribution grid are given in Section 4. Finally, the conclusions are drawn in Section 5.

2. BESS Components

Large-scale grid connected BESS is used to perform different tasks and applications in the power systems by using different control strategies and approaches. These applications are categorized and summarized in Table 1 [16]. The general structure of a BESS is depicted in Figure 1. The battery bank is the storage element that is comprised of multiple battery packs to store energy and discharge it when needed. Battery management system (BMS) is the combination of control devices that assure safe operation of the batteries. In the BESS, power electronic interfaces are designed to couple the battery units to the grid. A single dc-ac converter or the combination of dc-dc converter and dc-ac converter is utilized for controlling charging/discharging processes. The filter is generally utilized to reduce the harmonics at the power converter output. Transformer is needed in some applications to step-up output voltage of BESS to couple with the medium/high voltage level of the grid. If a multilevel converter topology is used, the transformer can be omitted due to high voltage output of the power converter. The other components such as switches and fuses are used for safe operation and the protection of the BESS. The most important BESS components are discussed thoroughly in this section.

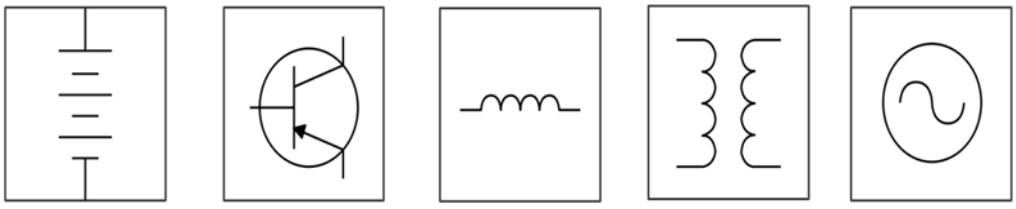

Fig. 1. The general structure of a BESS

International Journal of Energy Applications and Technologies, Year 2021, Vol. 8, No. 3, pp. 98-112

Table 1. BESS applications based on location in power system

Power supply side	Power grid side	Power distribution side
Smooth RES output fluctuations	Frequency regulation	Load leveling
Frequency regulation	Peak shaving	Power supply reliability
Standby power supply	System backup	Vehicle to grid application (V2G)
	Transmission and distribution networks upgrade deferral	Uninterruptible power supply (UPS)

2.1. Battery banks

Battery banks consist of multiple battery packs connected together. Each battery pack consists of numerous battery modules and each battery module includes several battery cells. The battery cell an electrochemical cell which is the core element in the BESS. The cell can store electrical energy in the form chemical energy and converts it back to electrical energy through reversible chemical reactions. This cell contains a positive electrode (cathode) and negative electrode (anode) immersed in the electrolyte to conduct ions between each other. The substances used in the electrodes differ based on the battery technology used. Figure 2 shows a schematic of the electrochemical cell in both charging and discharging operations. The charging/discharging of the battery cell are based on reduction and oxidation chemical reactions (redox in short) that occur at the electrodes. When the battery discharges, oxidation occurs at the anode and an electron is released and transferred through the electrolyte and accepted by the cathode through reduction. This electron transitions lead to the generation of electrical current. During charging operation, the same principle is applicable with reversed reactions while the battery is supplied by an external source [17]. The battery can be characterized by its capacity Q and open-circuit voltage (OCV). The capacity Q is given in Equation (1), where i is the battery current. Q is the highest possible energy quantity usually measured in coulombs that can be stored and extracted from the battery under certain circumstances depending on the battery volume, mass, and materials. The OCV is the potential difference between the battery electrodes when the battery is neither charging nor discharging. However, during charging and discharging, the measured voltage can be above or below OCV due to the polarization effect that is caused by chemical reactions and the internal components. Thus, the battery terminal voltage is a more precise characteristic parameter that accounts for the polarization effects. Another factor that influences the measured voltage of the battery is the SOC given in Equation (2), where Q_{max} is the maximum value of Q. The SOC is the rate of the current measured capacity compared to the original maximum capacity of the battery.

$$\boldsymbol{Q = \int i\, dt\ (1)} \tag{1}$$

$$\boldsymbol{SOC = 100 * \left(1 - \frac{Q}{Q_{max}}\right)} \tag{2}$$

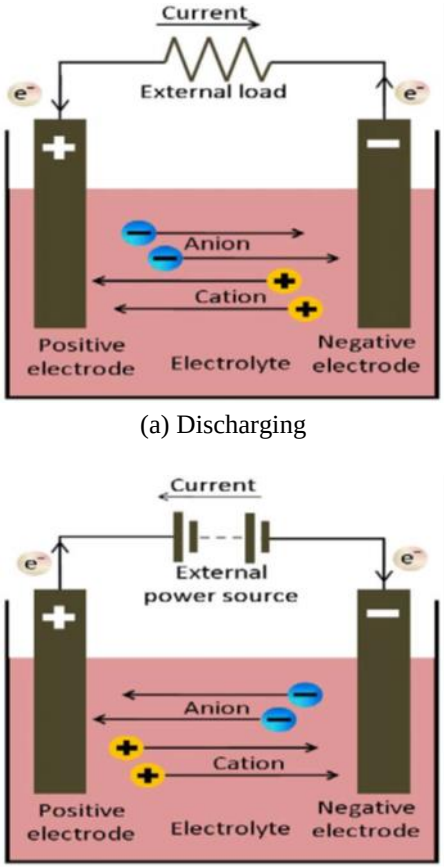

Fig. 2. The electrochemical cell structure and reactions during: (a) charging, (b) discharging [17]

2.2 Battery cell models

The modeling of the battery cell is necessary in order to capture the dynamics of the battery and extract and estimate some of vital parameters that affect the performance and efficiency of the battery such as state of health (SOH) and SOC. The battery models can be built and analyzed by different approaches. The most common models are electro-chemical models, mathematical models, and equivalent circuit models (ECM). Electrochemical modeling formulates a very precise description and relations of the battery parameters based on chemical reaction. However, it is very time consuming and has high complexity due to the non-linear differential equations to describe the battery characteristics. Mathematical model mainly focuses on building a mathematical relation between the battery voltage and current to predict and describe the battery behavior. The best commonly used mathematical model is the Shepherd

International Journal of Energy Applications and Technologies, Year 2021, Vol. 8, No. 3, pp. 98-112

model which is considered as a simple model compared to the other mathematical models with the same concept but includes more expressions and adjustments to make further improvement to the original model. In this model, the battery voltage V_B is defined as

$$\boldsymbol{V_B = E_o - K\left(\frac{Q}{Q-\int idt}\right) i - R_i i} \quad (1)$$

where E_o denotes the OCV, K is the polarization resistance and R_i is the internal resistance. m is linked to the losses from the internal resistance. ECM represents the dynamic and performance of the batteries using electrical circuit elements such as voltage source, current source, resistances, and capacitors. This model is capable of expressing the battery voltage as a function of SOC, current, and temperature under different charging and discharging conditions. In terms of computational accuracy and complexity, ECM falls between mathematical and electrochemical models. There is a variety of ECM models with different complexity levels depending on the electrical components included to capture certain dynamics. A simple model that includes only a voltage source connected to a resistor is shown in Figure 3.

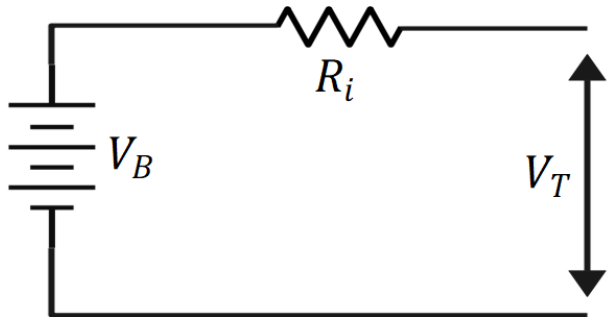

Fig. 3. A simple ECM model

In Figure 3, V_B is the OCV and V_T is the terminal voltage of the battery. The model has low accuracy due to its incapability to reflect the transient performance of the battery as it does not include a relationship between SOC and R_i. The Thevenin model shown in Figure 4 includes polarization components such as resistance R_p and capacitor C_p, which are connected in series with R_i. The addition of these components can reflect the transient performance of the battery at a certain SOC and capture terminal voltage dynamics, while the OCV is assumed to be constant. More RC networks can be added for further accuracy improvement in the polarization characteristic estimation. Thevenin based model is commonly adopted in the modeling of Li-ion batteries to extract battery parameters like SOC and SOH. Partnership for a New Generation of Vehicles (PNGV) model can capture the dynamics as a function of the load current by adding a capacitor C_b to the original Thevenin model as seen in Figure 5. In general, the accuracy of ECM models can be increased by including more circuit elements at the price of increasing the model complexity that can be a computation burden in large-scale BESS.

Figure 6 represents a generic battery model used in Matlab which is available in power systems library. This model can be used to model and simulate different kinds of secondary battery.

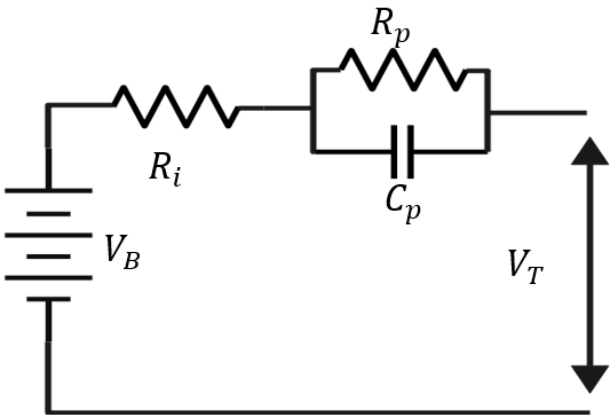

Fig. 4. Thevenin model

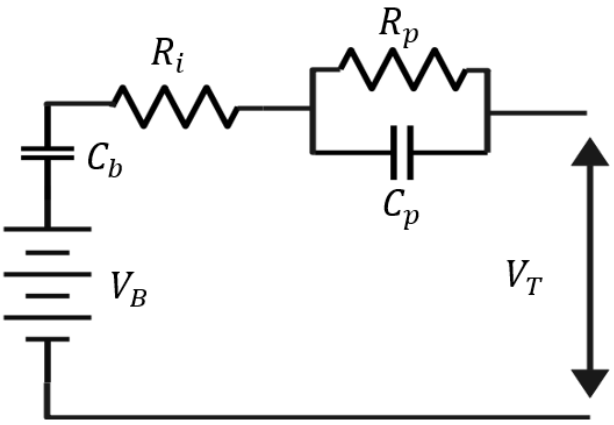

Fig. 5. PNGV model

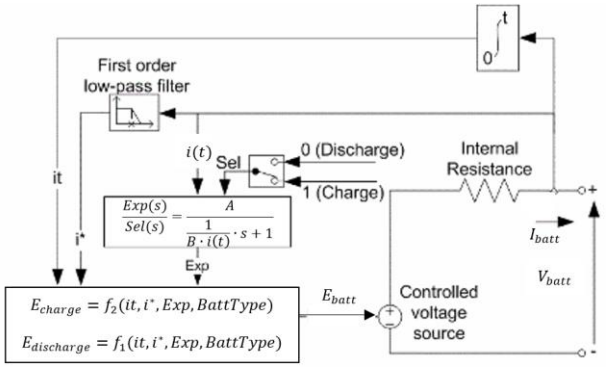

Fig. 6. The generic battery model used in Matlab

In this generic battery model, the charging and discharging battery voltages of a Li-ion battery can be represented as a function of current as follows

$$V_{Bdischarge} = E_o - K\left(\frac{Q}{Q-\int idt}\right) i - R_i i - K\left(\frac{Q}{Q-\int idt}\right) \int i\, dt + Ae^{-B\int idt} \quad (4)$$

International Journal of Energy Applications and Technologies, Year 2021, Vol. 8, No. 3, pp. 98-112

$$V_{Bcharge} = E_o - K\left(\frac{Q}{0.1Q+\int idt}\right)i - R_i i - K\left(\frac{Q}{Q-\int idt}\right)\int i\,dt + Ae^{-B\int idt} \quad (5)$$

where A is the exponential voltage and B is the exponential capacity in Ah^{-1}. Compared to the Shepherd model two additional terms are added. In Equations (4) and (5), the fourth term represents the polarization characteristics associated with the overvoltage. This term along with E_o can realize a better relation for the non-linearity of OCV corresponding to the SOC. The fifth term denotes dynamic voltage that exponentially changes with SOC and can be illustrated as discharge curves given in Figure 7 in order to represent the non-linear hysteresis occurrence between charging and discharging.

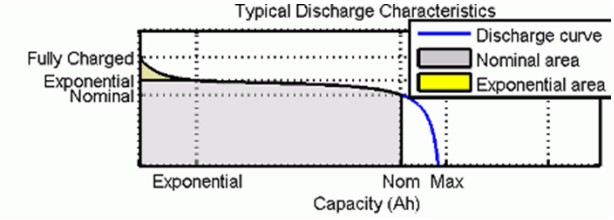

Fig. 7. Generic battery model discharge curve

The model given by Equations (4) and (5) assumes that R_i is constant during charging/discharging cycles and does not change with the current amplitude. The ideal case is assumed where the characteristics of both charging/discharging processes are the same and the parameters are extracted from the discharge characteristics. The Peukert effect is negligible as the capacity does not vary with the current amplitude. On the other hand, the self-discharge is negligible since it can be derived by placing large resistance in parallel with the battery terminals. Also, the battery memory effect is not considered. Based on these assumptions, the generic battery model in Matlab can be favorable when the aforementioned effects and characteristics are not a matter of concern. This model can also be preferred in large-scale BESS applications where tremendous number of battery cells is included.

2.3 Battery pack models

Large battery banks are formed by connecting multiple battery packs that contain multiple modules of cells connected either in series or parallel as shown in Figure 8. Multiple cells are connected in series to obtain larger voltage level by adding up the voltage of each cell and in parallel to stack up higher capacity. When multiple cells are connected in series as shown in Figure 9, the voltage of each cell is added up to calculate the overall OCV (OCV_{series}) as expressed in Equation (6), where m is the number of the cells connected in series and OCV_j is the OCV of the j^{th} cell. Equation (7) shows the total internal resistance ($R_{i,series}$) when multiple cells are connected in series, where $R_{i,j}$ denotes the R_i of the j^{th} cell. Equation (8) shows the total equivalent polarization resistance ($R_{p,series}$) when multiple cells are connected in series, where $R_{p,j}$ denotes the R_p of the j^{th} cell. The equivalent capacity ($C_{n,series}$) of the multiple cells connected in series is shown in Equation (9). As seen, $C_{n,series}$ is equal to the capacity of each cell ($C_{n,j}$). This is true if all cells are identical. However, in real case, the variation in cell capacity always exists due to manufacturing diversity. Hence, the cell with the lowest capacity determines the capacity of the entire string. Series connected cells discharge at the same rate until it reaches the cut-off voltage. Nevertheless, this cut-off voltage is limited by the cut-off voltage of the weakest cell in such a way that only the weakest cell reaches its cutoff voltage. The terminal voltage ($V_{Tseries}$) of the series battery string can be defined in Equation (10), where V_p is the polarization voltage across the RC network.

$$OCV_{series} = mOCV = OCV_1 + OCV_2 + \cdots + OCV_m \quad (6)$$

$$R_{i,series} = mR_i = R_{i,1} + R_{i,2} + \cdots + R_{i,m} \quad (7)$$

$$R_{p,series} = mR_p = R_{p,1} + R_{p,2} + \cdots + R_{p,m} \quad (8)$$

$$C_{n,series} = C_{n,1} = C_{n,2} = C_{n,m} \quad (9)$$

$$V_{Tseries} = mV_T = m(OCV - V_p - R_i i) \quad (10)$$

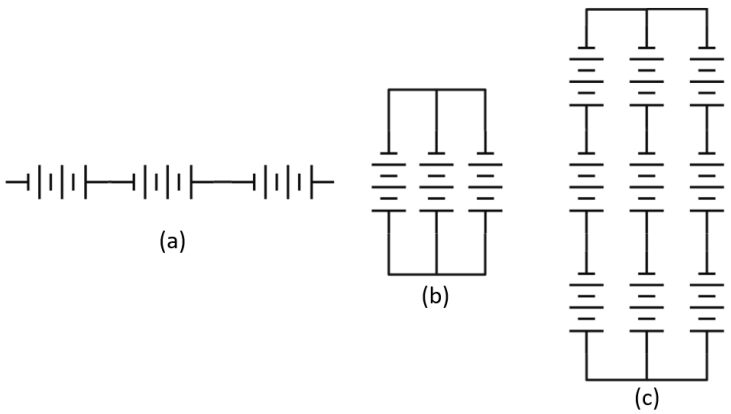

Fig. 8. Battery cell connections: (a) series connection, (b) parallel connection, (c) series/parallel connections

International Journal of Energy Applications and Technologies, Year 2021, Vol. 8, No. 3, pp. 98-112

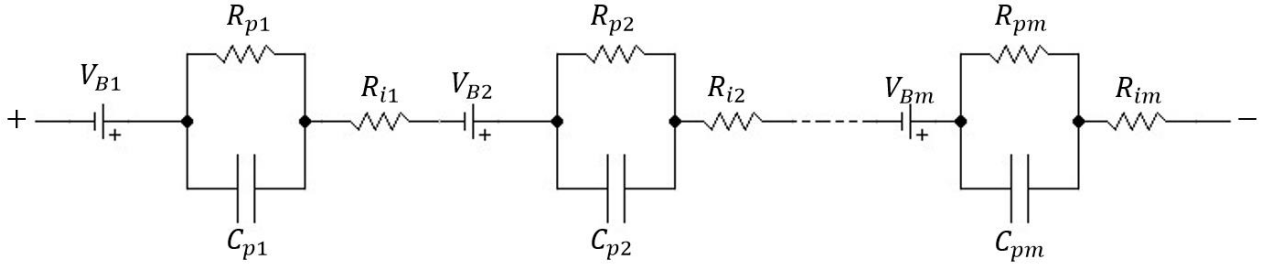

Fig. 9. The model of series connected battery cells

Figure 10 depicts the model of parallel connected battery cells. In parallel connection, the OCV of each battery cell is equal to each other as shown in Equation (11). The equivalent internal resistance of parallel connected battery cells ($R_{i,parallel}$) is given in Equation (12), where n is the number of parallel connected cells. On the other hand, the equivalent polarization resistance ($R_{p,parallel}$) and capacitance ($C_{n,parallel}$) of parallel connected battery cells are given in Equation (13) and (14), respectively. The terminal voltage V_T in the parallel configuration can be expressed in Equation (15) as a function of the open circuit voltage OCV, the current flowing through each parallel connected cell i_k , and the n number of parallel connections. Evidently, the terminal voltage is inversely proportional to the number of parallel connected cell as it decreases with more cells connected in parallel. The discharge current rate in parallel connected cell is unequal and expressed as a decreasing function of the output voltage.

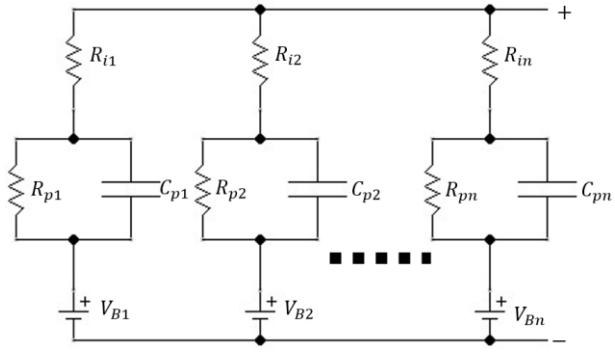

Fig. 10. The model of parallel connected battery cells

$$OCV_{parallel} = OCV_1 = OCV_2 = OCV_m \quad (11)$$

$$R_{i,parallel} = \frac{R_i}{n} = \left(\frac{1}{R_{i,1}} + \frac{1}{R_{i,2}} + \cdots + \frac{1}{R_{i,n}}\right)^{-1} \quad (12)$$

$$R_{p,parallel} = \frac{R_p}{n} = \left(\frac{1}{R_{p,1}} + \frac{1}{R_{p,2}} + \cdots + \frac{1}{R_{p,n}}\right)^{-1} \quad (13)$$

$$C_{n,parallel} = nC_n = C_{n,1} + C_{n,2} + \cdots + C_{n,} \quad (14)$$

$$OCV - \frac{OCV}{n} + \frac{V_T}{n} = OCV - \frac{V_p}{n} - \frac{R_i}{n} i_k \quad (15)$$

In order to obtain safe and optimum performance of the battery, a multi-cell battery model should be built to reflect the characteristics of voltage, capacity, and the current distribution between cells. Moreover, these characteristics depend on several factors such as connections of the cells, cell-to-cell variations, and discharge current rate [18]. In the literature, battery packs are usually modelled using one of three methods. The first method involves constructing a cell model and then accumulating series and parallel cell structures to create a pack model. The second method involves converting the cell model into a simplified battery pack model that is similar to the cell model. The third method proposes a battery pack model that encompasses all aspects of the battery pack [19]. The cell-to-cell variation is a serious dilemma in batteries that could cause SOC imbalance between the batteries by limiting the available capacity and reduces the lifetime of the batteries. The study in [20] presents a screening method that is used to sort the battery cells with similar characteristics together to minimize the effects of cell variations. This can be done over two steps. In the first step, the cells with similar discharging capacities are grouped after being measured several times at different discharge current rates. In the second step, the selected cells from the first step are subjected to pulse-type charging/discharging current at a diversity of SOC points to choose cells that have similar variances. After the screening process is applied, the battery pack can be modelled by extending the model from single cell to multi-cell battery such that the parameters of the battery pack for series string of simple or Thevenin multi-cell models can be expressed. Battery packs with series connected cells suffer from a serious reliability issue since a fault in a single cell causes the entire pack to cease operation. On the other hand, parallel connected cells is able to continue its operation even during a fault in a single cell, but the imbalance of the charging/discharging current rates among the cells could lead to cells mismatch. A battery pack having cells connected both in series and parallel can be considered as a more robust design with all the features of the series and parallel connectivity. However, this arrangement is also accompanied with all their drawbacks for example a single fault will cause failure in one series string but the rest of parallel connected strings will be unaffected. Also, the battery pack capacity will also be limited by the weakest cell.

2.4 Cell arrangements

There is a variety of connection topologies for the series/parallel battery pack models depending on the wiring order of the series and parallel modules and the cell arrangements inside the pack. The most common topologies are the parallel cell module (PCM) and series cell module (SCM) named by Plett and Klein [18]. In PCM, the cells are wired in parallel forming modules of parallel connected cells then the modules are wired in series. As a result, this approach is able to ease out any variation in the resistance and capacities of the cells such that the battery pack continuously operate even with significant parameters variation. If a single cell introduces leakage current a fault can occur. The battery can still be functional but with less terminal voltage amplitude in case of short-circuit fault in a single cell as all cells in the module are affected by the same fault. SCM, on the other hand, first connects the cells in series then the modules are wired in parallel. This configuration allows the modules to self-balance when no load is connected. When a single cell is subjected to open-circuit fault, the entire string associated with the faulty cell is disconnected from the pack. Whereas, a short-circuit fault in a single cell subjects all the cells in the same string to higher voltage in order to keep up with the bus voltage of the battery pack. The study in [18] involves 4 different cells connection topologies including SCMs and PCMs, as shown in Figure 11. It focus on inspecting the relationship between the maximum capacity of the battery and the cells arrangement in case of mismatch in the cells parameters. It is then found out that the battery pack with PCM arrangement provides higher capacity and reduces the statistical dispersion. Also, it is highlighted that the battery pack capacity can be even lower than the weakest cell and the first cell to reach the cut-off voltage is not necessarily the weakest cell. There is extensive number of arrangements for wiring the cells inside the battery pack. The appropriate arrangement of the cells is critical such that different arrangements can lead to huge variation in the capacity of the battery pack. The number of possible arrangements n can be estimated based on the number of parallel connections p having s cells as follows

$$n = \frac{(p*s)!}{p!(s!)^p} \tag{16}$$

The charging of the battery considering different cell arrangements in the battery pack is studied in [21]. In that study, 3 Li-ion battery cells with different initial SOC values are connected to a charger to deliver a constant current and voltage needed to charge the battery pack. When the battery cells are connected in series, to ensure the charging speed of the Li-ion battery pack, it is first charged by constant current, as the terminal voltage exceeds the threshold voltage. The charger switches to charging by constant voltage as soon as one of the cells reaches 100% of its nominal capacity. Additionally, the charging stops to prevent over charging. Even though the series charging can achieve fast charging with consistent charging current, the battery cells are more vulnerable to SOC imbalance that could limit the overall capacity of the battery pack. This situation can also lead to overcharging or undercharging. In a similar manner, when the parallel connected cells are subjected to parallel charging, the charging current is distributed between the cells based on their SOC, as the cell with the lowest capacity is charged with higher current amplitude. Such an action realizes better energy balance in the battery pack, but at the cost of increasing the polarization effects. Later, a comprehensive approach is proposed that can realize both series and parallel charging to achieve fast charging and energy balance in the battery pack by adding switching devices across the battery terminals to interchange between the two charging modes.

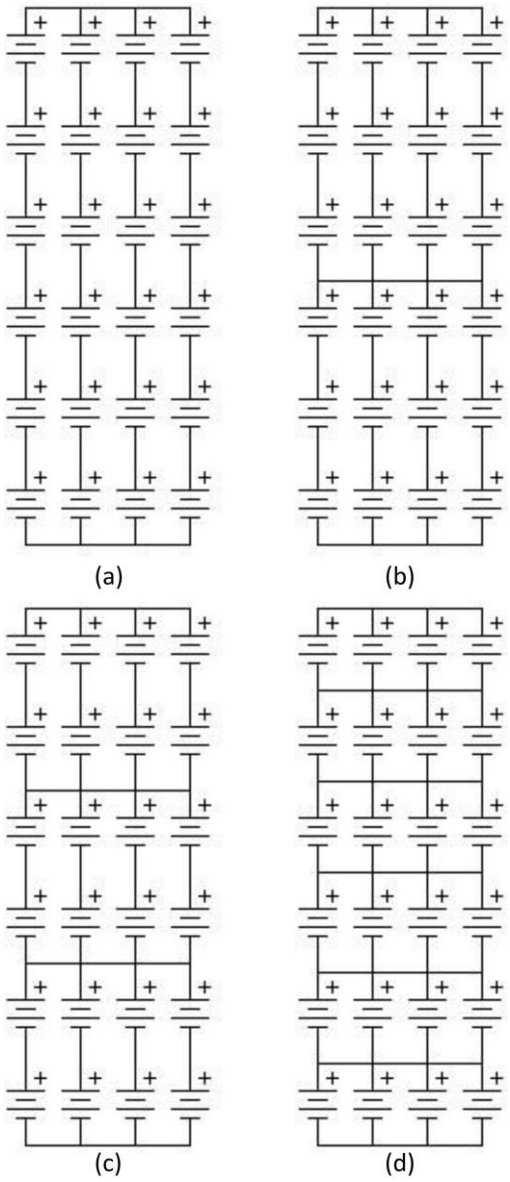

Fig. 11. Different battery module arrangements

The charging of the battery considering different cell arrangements in the battery pack is studied in [21]. In that study, 3 Li-ion battery cells with different initial SOC values are connected to a charger to deliver a constant current and voltage needed to charge the battery pack. When the battery cells are connected in series, to ensure the charging speed of the Li-ion battery pack, it is first charged by constant current, as the terminal voltage exceeds the threshold voltage. The charger switches to charging by constant voltage as soon as one of the cells reaches 100% of its nominal capacity. Additionally, the charging stops to prevent over charging. Even though the series charging can achieve fast charging with consistent charging current, the battery cells are more vulnerable to SOC imbalance that could limit the overall capacity of the battery pack. This situation can also lead to overcharging or undercharging. In a similar manner, when the parallel connected cells are subjected to parallel charging, the charging current is distributed between the cells based on their SOC, as the cell with the lowest capacity is charged with higher current amplitude. Such an action realizes better energy balance in the battery pack, but at the cost of increasing the polarization effects. Later, a comprehensive approach is proposed that can realize both series and parallel charging to achieve fast charging and energy balance in the battery pack by adding switching devices across the battery terminals to interchange between the two charging modes.

2.5 Battery management system

The general structure of a battery management system (BMS) is illustrated in Figure 12. BMS can be embedded with each battery cell, module, or pack to ensure safe and optimal operation of the batteries under different operating conditions. BMS is mainly used for thermal management and prevent battery degradation by providing protection against overcharging and undercharging. The control strategy used in the BMS are decided based on the measured battery parameters such as voltage, current, and temperature in order to meet the power demand from the energy management system [22]. BMS can improve BESS performance in various ways by performing different objectives such as, optimizing charging/discharging, SOC and SOH estimation and monitoring, SOC balancing, current, voltage, and temperature monitoring for individual cells and battery packs, and protection against capacity fade and internal degradation. In large-scale BESS, BMS of each battery pack is merged to form a collective management system that optimizes the entire BESS [23].

2.6 Filter and transformer

A filter is usually the combination of L and C components used to mitigate the harmonics associated with high-frequency switching in power converters. The filter can be connected to the input, output, or both of the power converters. In a BESS application, as the simplest case, a single choke inductor connected with a resistance, or an advanced type such as LCL filter can be arranged. On the other hand, a transformer is essential for grid-connected BESS applications to step-up or step-down the voltage level of the BESS output. The transformer sizing and rating depend on the scale of the BESS and the topology of the power electronic converters being used. The transformer is usually required for two or three level converters. But in case when multi-level converters are utilized, a transformer connection is not generally necessary, as higher voltage level can be attained at the converter output. Also, with the use of multi-level converter topology in BESS applications, the transformer rating and size can be reduced to couple with medium voltage networks, hence the costs are reduced.

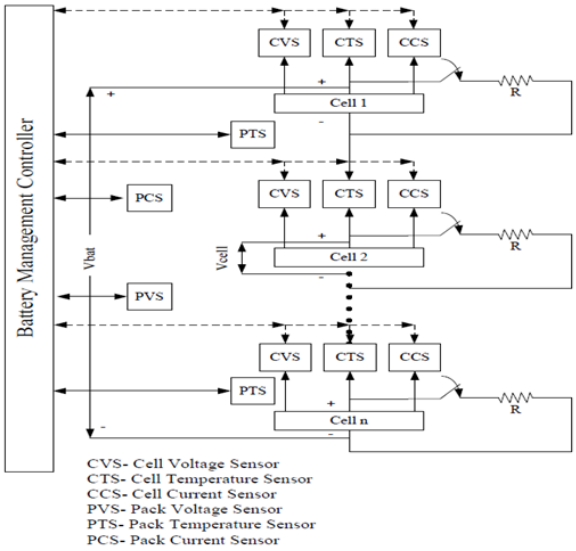

Fig. 12. General schematic of BMS [22]

2.7 Power conversion system

Power conversion system (PCS) in BESS consists of one or more power electronic converters mainly 1) to charge and discharge the batteries, 2) to provide electrical isolation, and 3) to control real and reactive power in both directions to meet grid regulations. There are many types of power electronic converter topologies in BESS applications. The basic type of PCS is a single-stage two-level voltage source converter (VSC) to convert the dc voltage of the batteries into ac voltage during discharging and ac voltage to dc voltage during discharging. On the other hand, two-stage PCS includes a dc-dc buck-boost converter to step-up the voltage of the battery packs and an inverter. For grid scale BESS applications that require high-voltage level and large power, the battery packs are divided among multiple power modules that are comprised of a multi-level converter such as neutral point clamp converter, MMC or CHB converter. Another advantage of using multi-level converter is that the BESS

output can be directly coupled to the grid without the need of a transformer. The CHB converter shown in Figure 13 is more suitable for BESS applications as it is capable of achieving SOC balance by charging and discharging the H-bridge modules in different rates with simple control strategies. Moreover, if any fault occurs either in the storage unit or the converter side, the faulty power module can be easily bypassed without affecting the output power and voltage. The number of voltage levels in a CHB converter topology n depends on the number of CHB cells N, as expressed in Equation (17). The required N is calculated in Equation (18), where V_{LL} is the line-to-line rms voltage of the grid and V_{dc} is the dc link voltage of the BESS.

$$n = 2N + 1 \tag{17}$$

$$N \geq \frac{\sqrt{2}V_{LL}}{\sqrt{3}V_{dc}} \tag{18}$$

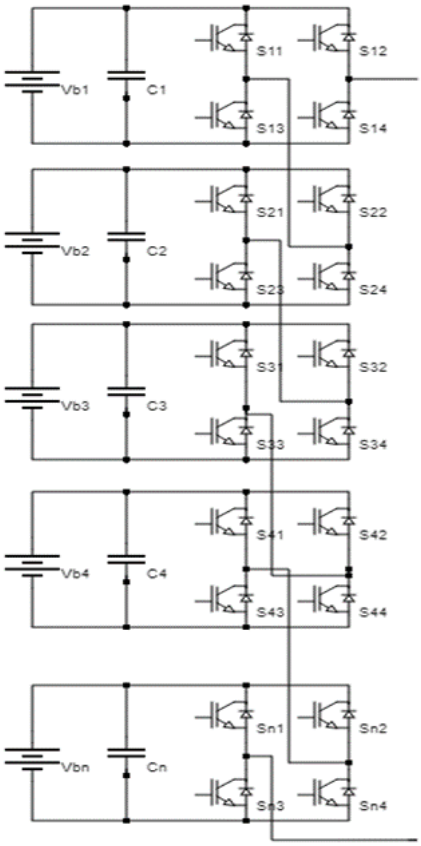

Fig. 13. CHB topology

By utilizing Equation (17) and (18), N is calculated as 5 for a 1 MWh BESS connected to three-phase grid with a point of common coupling (PCC) voltage of 4.16 kV. In such a design, n is 11 for a dc link voltage of 780V. Compared to two-level VSC topology, the number of series battery connections are reduced when CHB topology is used, so the reliability of the system increases. The number of series battery connections can be further reduced by connecting a bidirectional buck-boost dc-dc converter to each CHB cell, as shown in Figure 14.

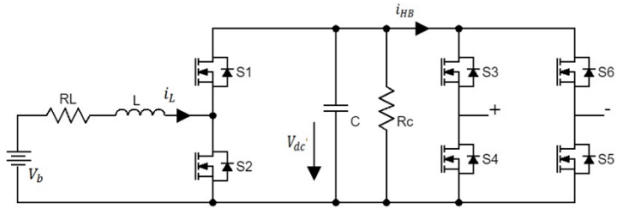

Fig. 14. Bidirectional DC-DC converter connected to CHB cell

With this configuration, dc-link voltage can be controlled and consequently the charging/discharging of the batteries can be easily controlled. However, using more power electronic components increase the cost and losses associated with the switching devices. Further, BESS control becomes more complex. Considering LiFePo4 battery module specified in Table 2, a comparison between single stage CHB, two-stage CHB, and two-level VSC is given in Table 3 in terms of number of battery connections required to implement 1MWh capacity BESS connected to grid at the PCC voltage of 4.16 kV. The number of battery modules used in each battery pack is the least in two-stage CHB design. However, the total number of modules used in both single and two-stage CHB is more than two-level one. The dc-dc converter gives more freedom in the design of the battery pack voltage and reduces the number of series connections in exchange for more parallel connections. Hence, the reliability of the overall system is increased at the cost of additional switching devices as well as switching losses.

Table 2. Battery parameters

Battery type	Lithium Ferro Phosphate (LiFePo4 – LFP)
Voltage min. / nom. / max.	44.0 V / 51.2 V / 58.4 V
Energy stored	2.56 kWh / 50 Ah
Number of cells per module	16

Table 3. Battery and switching devices needed in BESS

Design type	Total modules in BESS	Total cells in BESS	Series connections per pack	Parallel connections per pack	Switching devices in BESS
VSC	390	6240	65	2	6
CHB	450	7200	15	2	60
CHB-dc/dc	450	7200	10	3	90

International Journal of Energy Applications and Technologies, Year 2021, Vol. 8, No. 3, pp. 98-112

3. BESS Control

There are various control strategies available in the literature to control BESS depending on the BESS structure, power electronic converters used, and the desired application. Generally, the power flow of the BESS is controlled by regulating the power electronic converters that interfaces the BESS with the grid or load. A control strategy presented in [24] is based on recurrent neural networks to integrate BESS with RES. A nonlinear control approach based on feedback linearization is proposed in [25] to control grid-connected BESS. In [26], a cascaded control scheme based on PQ control is adopted to regulate a grid-connected BESS. The study in [5] conducts a comparison between PQ control and vector oriented current control through simulation for a grid-connected BESS. The results show that the current vector control gives more promising results than PQ control under different charge rates. The voltage equations for the grid-connected BESS shown in Figure (15) is

$$V_{abc} = V_{iabc} - L_f \frac{di_{abc}}{dt} - R_f i_{abc} \quad (2)$$

where V_{abc} and V_{iabc} are three-phase the grid and inverter output voltages, respectively, L_f and R_f is the filter inductance and resistance, respectively, i_{abc} are three-phase currents. In order to apply *dq* current control, the expression in Equation (19) has to be transformed from stationary *abc* coordinates to the synchronous rotating *dq0* coordinates by applying Park transformation to acquire the following expressions [27]:

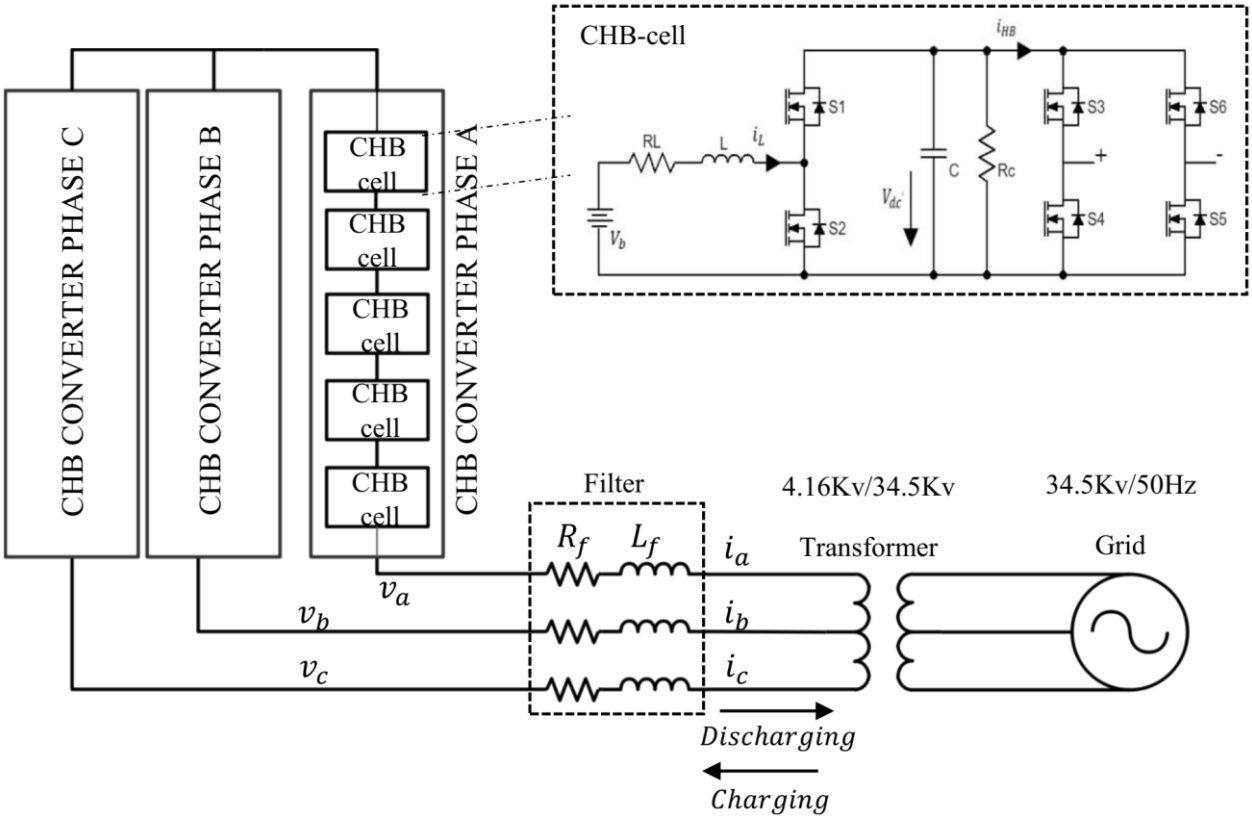

Fig. 15. Grid connected CHB based BESS

$$V_d = V_{id} + L_f \omega i_q - L_f \frac{di_d}{dt} - R_f i_d \quad (3)$$

$$V_q = V_{i_q} - L_f \omega i_d - L_f \frac{di_q}{dt} - R_f i_q \quad (4)$$

where V_d and V_q is the *d-axis* and *q-axis* components of grid voltage, respectively, V_{id} and V_{iq} is the *d-axis* and *q-axis* components of the inverter output voltage, respectively, i_d and i_q is the *d-axis* and *q-axis* components of phase currents, respectively, and ω is the grid angular frequency. Equation (20) and (21) can be used to control the active and reactive power of the BESS independently. Figure 16 shows PI based decoupled current control scheme. The current references ($i_d *$, $i_q *$) are calculated according to the desired active and reactive power to generate the voltage reference signals for the inverter (V_{Md}, V_{Mq}), respectively.

Decoupled current control scheme relies on the alignment of the inverter voltage phasor with the reference phase angle θ of the grid. A common way to track the grid phase angle θ is to use a phase locked loop.

A bidirectional dc-dc converter can be connected to the battery side to regulate the charging/discharging processes, step-up the voltage, and stabilize the dc-link voltage. This is

done by regulating the dc-link voltage and the inductor current in a cascaded manner such that the inner loop of the inductor current is at least ten times faster than the outer control loop of the dc-link voltage. The cascaded PI control scheme of dc-dc converter is shown in Figure 17. The dc-dc converter can be switched to operate in boost mode to discharge the batteries, or in buck mode to charge the batteries.

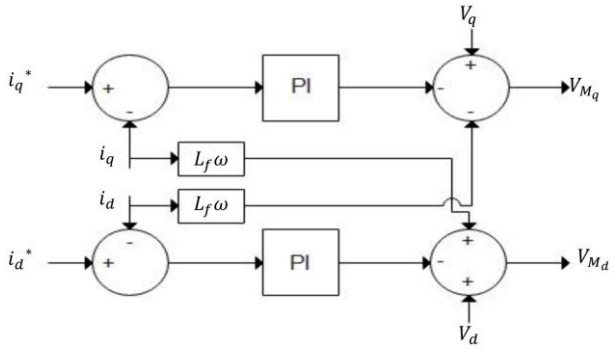

Fig. 16. PI based decoupled current control scheme

A bidirectional dc-dc converter can be connected to the battery side to regulate the charging/discharging processes, step-up the voltage, and stabilize the dc-link voltage. This is done by regulating the dc-link voltage and the inductor current in a cascaded manner such that the inner loop of the inductor current is at least ten times faster than the outer control loop of the dc-link voltage. The cascaded PI control scheme of dc-dc converter is shown in Figure 17. The dc-dc converter can be switched to operate in boost mode to discharge the batteries, or in buck mode to charge the batteries.

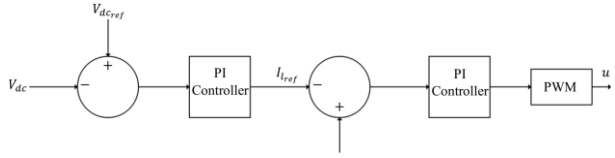

Fig. 17. Cascaded PI control scheme of dc-dc converter

4. Simulation Studies

A simulation test is performed on 1MWh CHB-BESS shown in Figure (15) In this design, decoupled current control is adopted to regulate the CHB and control the power flow between the grid and BESS, and bi-directional buck-boost converters is embedded to each battery storage unit and controlled by cascaded PI control to regulate the charging/discharging of the batteries. The simulation is conducted over a total period of 2 seconds to test the capability of the BESS to exchange active and reactive power with the grid. The parameters of the grid-connected BESS for the simulation study are listed in Table 4. Figure 18 shows that the simulation starts by drawing 1 pu active power from the grid for half a second by controlling the synchronous rotating currents i_d and i_q, while the reactive power reference is set to zero. Zero reactive power ensures unity power factor operation of the BESS. At t=0.5 seconds, the power flow is reversed and the BESS starts supplying 1 pu of active power to the grid while reactive power set point is still zero. When a duration of 1 second has elapsed, the power flow is reversed again and the active power reference is set to 0.5 pu, while the reactive power reference is set to -0.5 pu. At the last half-second of the simulation, both the active power and reactive power flow is reversed with the same amplitude. The transients recorded in Figure 18 verify that the decoupled current controller is able to successfully track the desired active and reactive power references with minimum error.

Table 4. The parameters of the grid-connected BESS

Parameter	Symbol	Value
Grid line-to-line voltage	$V_{g,LL}$	34.5 kV
Grid frequency	f_g	50 Hz
PCC line-to-line voltage	$V_{i,LL}$	4.16 kV
CHB rated power	P_{rated}	1 MW
Filter resistance	R_f	3.14 mΩ
Filter inductance	L_f	0.5 mH
Battery voltage	V_b	461 V
dc-link capacitance	C_{dc}	5 mF
Capacitor internal resistance	R_{dc}	10 kΩ
Energy storage cell inductance	L	0.5 mH
Inductance internal resistance	R_L	0.1 Ω
CHB switching frequency	f_{sw}	2 kHz
dc-dc converter switching frequency	f_{dc-dc}	10 kHz

Figure 19 shows voltage and current waveforms at the PCC. The battery dynamics of an individual battery storage unit in a selected CHB cell are demonstrated in Figure 20. During the half-second period when the BESS is drawing active power from the grid, the battery starts charging as SOC is increasing and the battery current is negative. At t=0.5 seconds, the active power flow is reversed and the battery starts discharging with positive current. Similarly, at t=1 second, the power flow is reversed and the amplitude of the active power reference is reduced to its half value so is the battery current. At the last period, the battery starts discharging and injects active power into the grid according to the active power reference. Observably, due to the DC-DC converter switching the battery exhibit pulsating charging and discharging that slightly increase and decrease the battery voltage during charging and discharging respectively. Moreover, the pulsating charging/discharging of the batteries naturally introduces current ripples throughout the operation which has no negative impact on battery ageing according to the study done in [28].

International Journal of Energy Applications and Technologies, Year 2021, Vol. 8, No. 3, pp. 98-112

During the last second when BESS starts injecting and drawing reactive power from the grid there is no significant effect on the battery dynamics compared when the reactive power is zero at the first second of the simulation. The voltage of the battery is nearly constant throughout the operation of the BESS with small oscillations around 1% of its nominal value. The dc-link voltage reference is set to 780 V as seen in Figure 21. The bidirectional dc-dc converter was able to maintain the dc-link voltage fixed at the desired value with voltage ripples less than 1% of the nominal voltage throughout the simulation under different operating conditions.

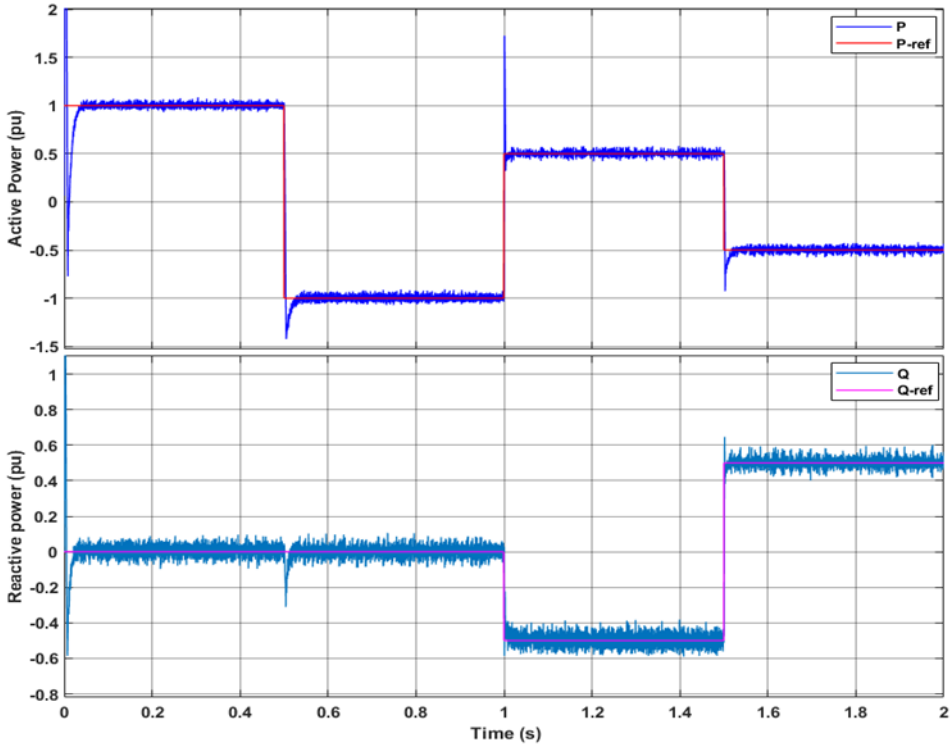

Fig. 18. Active and reactive power response

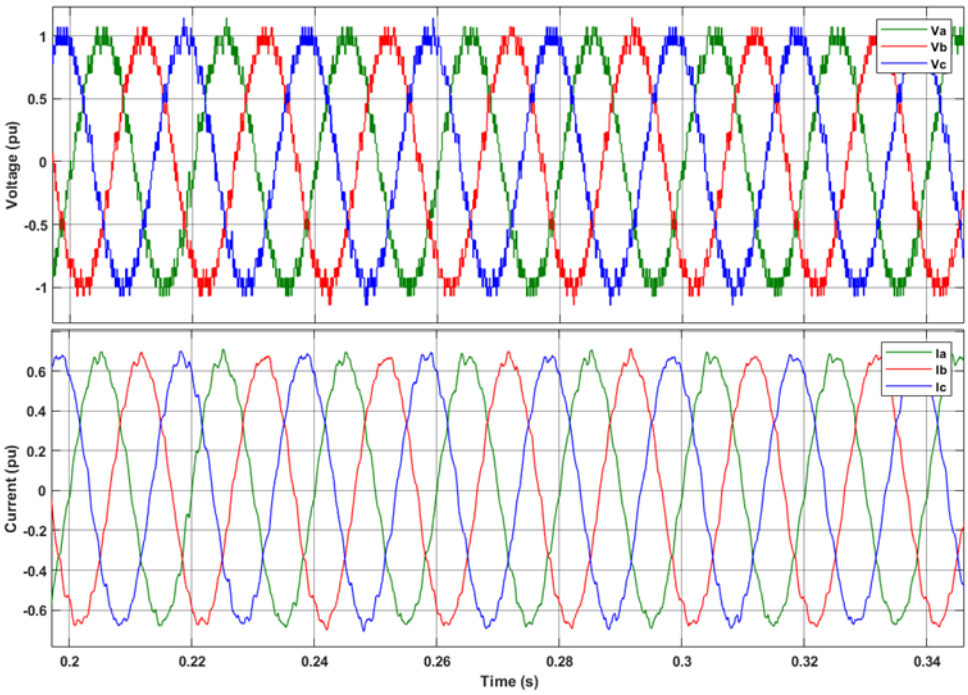

Fig. 19. Voltage and current waveforms at PCC

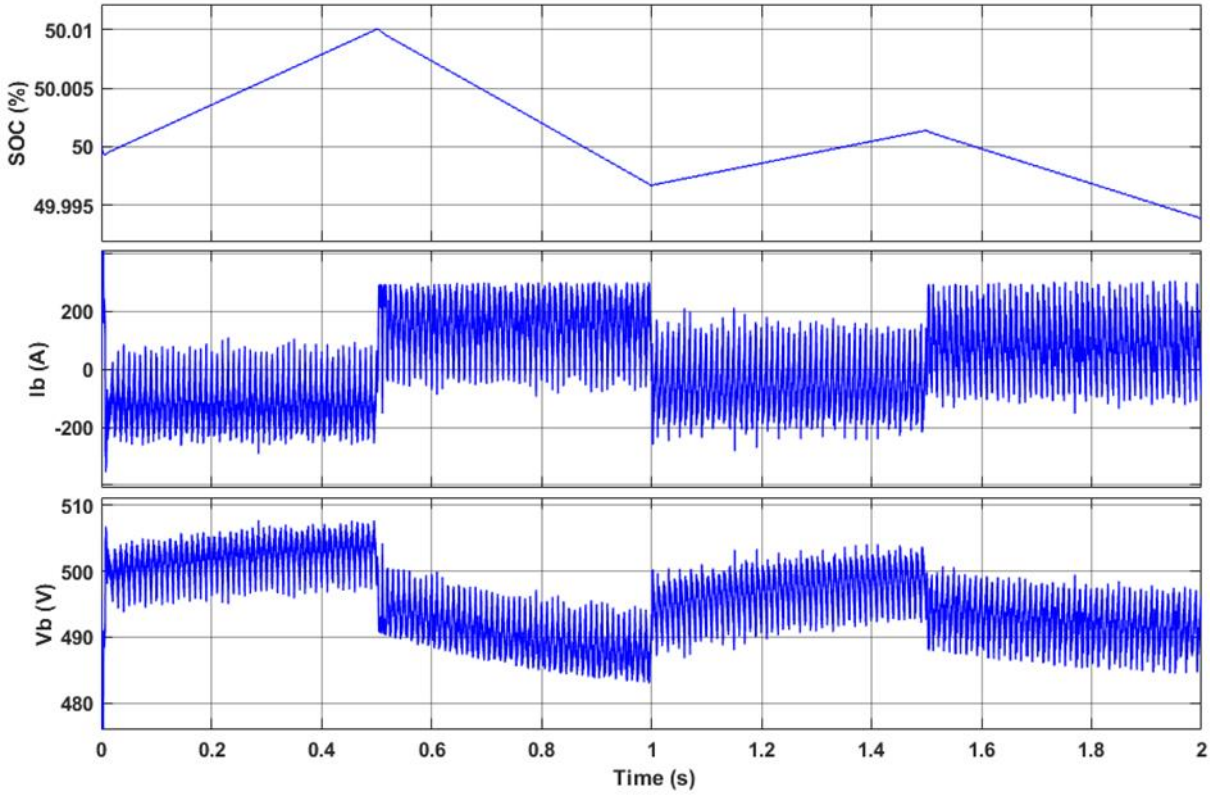

Fig. 20. The battery dynamics

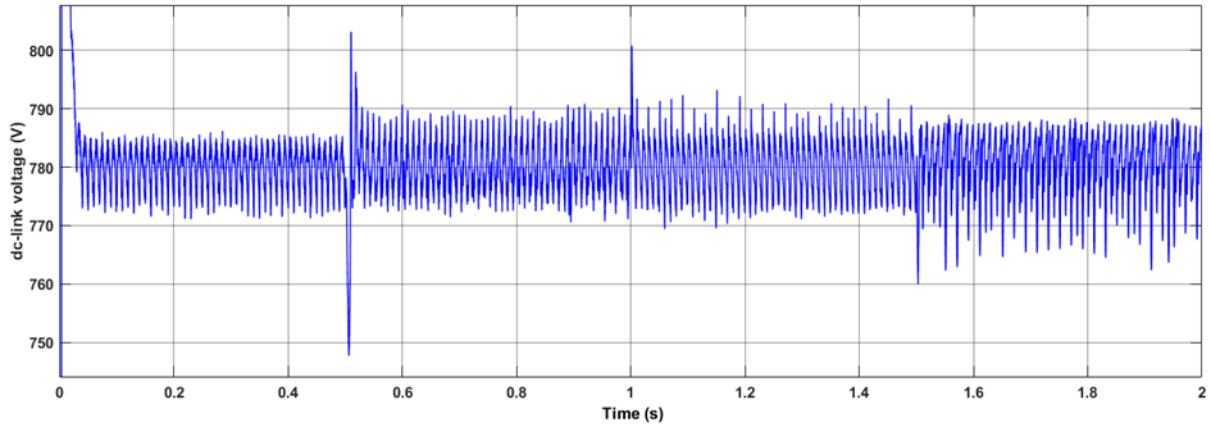

Fig. 21. DC-link voltage

5. Conclusions

This paper first gives a summarized overview of the BESS components focusing on the different models and design of the battery structure from different perspectives. Different battery cell types, different modeling approaches along with the cell arrangements inside the battery pack are discussed. In order to model the battery with reasonable precision and acceptable computational requirements, first the model has to be chosen according to the study needs and then considering the scale of the battery model, only the parameters of interests have to be included in the model. In the second part of the paper, a simulation study of a grid-connected 1 MWh BESS is presented with some simulation results. In simulation, the battery block model is used without including the parameters such as, temperature, self-discharge, battery ageing, and battery memory effect which are irrelevant to this study. The simulation results demonstrated acceptable transient performance of the designed controllers in tracking the active and reactive power references by charging and discharging the batteries.

ORCID

Y.M.S. Al-khdhairi 0000-0001-9580-0497

A. M. Vural 0000-0003-2543-4019

References

[1] Bae, A., Choi, S., Kim, J., Won, C., and Jung, Y. 2014. LiFePO4 dynamic battery modeling for battery simulator, 2014 IEEE International Conference on Industrial Technology (ICIT), 26 Feb.-1 March 2014, Busan, Korea (South), pp. 354-358.

[2] Alshehri, J., Alzahrani, A., and Khalid, M., 2019. Voltage and Frequency Control of Microgrids With Distributed Generations and Battery Energy Storage, 2019 8th International Conference on Renewable Energy Research and Applications (ICRERA), 3-6 Nov, Brasov, Romania, pp. 381-385.

[3] Miller, N., Manz, D., Roedel, J., Marken, P., and Kronbeck, E., 2010. Utility scale Battery Energy Storage Systems. IEEE PES General Meeting, 25-29 July, Minneapolis, MN, USA, pp. 1-7.

[4] Zhou, X., Lin, Y., and Ma, Y., 2015. The overview of energy storage technology, 2015 IEEE International Conference on Mechatronics and Automation (ICMA), 2-5 Aug, Beijing, China, pp. 43-48.

[5] Sarah, A., and Ray II, W., and Bayne, S., (2014). Comparison study of the controllers for grid connected battery system, 27-28 Oct, Ronkonkoma, NY, USA, p1-6.

[6] Subburaj, A. S., and Bayne, S. B., 2014. Analysis of dual polarization battery model for grid applications, 2014 IEEE 36th International Telecommunications Energy Conference (INTELEC), 28 Sept-2 Oct, Vancouver, BC, Canada, Pp. 1-7.

[7] Moo, C., Ng, K. S., and Hsieh, Y., June 2008. Parallel Operation of Battery Power Modules, in IEEE Transactions on Energy Conversion, vol. 23, no. 2. pp. 701-707.

[8] Moo, C., Ng, K. S., and Hu, J. 2009. Operation of battery power modules with series output, 2009 IEEE International Conference on Industrial Technology, 10-13 Feb, Churchill, VIC, Australia, pp. 1-6.

[9] Chen, F., Qiao, W., and Qu, L., 2017. A modular and reconfigurable battery system, 2017 IEEE Applied Power Electronics Conference and Exposition (APEC), 26-30 March, Tampa, FL, USA, pp. 2131-2135.

[10] Ci, S., Lin, N., and Wu, D., 2016. Reconfigurable Battery Techniques and Systems: A Survey, in IEEE Access, vol. 4. pp. 1175-1189.

[11] Schroeder, M., Henninger, S., Jaeger, J., Raš, A., Rubenbauer, H. and Leu, H., 2013. Integration of batteries into a modular multilevel converter, 2013 15th European Conference on Power Electronics and Applications (EPE), 2-6 Sept, Lille, France, pp. 1-12.

[12] Tian, K., Ali, S., Huang, Z., and Ling, Z., 2019. Power control and experiment of 2MW/10kV cascaded H-bridge power conversion system for battery energy storage system, 8th Renewable Power Generation Conference (RPG 2019), 24-25 Oct, Shanghai, China, pp. 1-7.

[13] Zhi-Bin, L., Yang, C., Qin-Dong, M., Hai-Feng, G., Bai-hua, Z., and Zhi-Gang, L., 2014. Design of 2MW/10kV cascaded power conversion system, IECON 2014 - 40th Annual Conference of the IEEE Industrial Electronics Society, 29 Oct-1 Nov, Dallas, TX, USA, pp. 4250-4255.

[14] Baruschka, L., and Mertens, A., 2011. Comparison of Cascaded H-Bridge and Modular Multilevel Converters for BESS application, 2011 IEEE Energy Conversion Congress and Exposition, 17-22 Sept, Phoenix, AZ, USA, pp. 909-916.

[15] Chatzinikolaou, E., and Rogers, D. J., September 2017. A Comparison of Grid-Connected Battery Energy Storage System Designs, in IEEE Transactions on Power Electronics, vol. 32, no. 9. pp. 6913-6923.

[16] Li, X., and Wang, S., 2019. A review on energy management, operation control and application methods for grid battery energy storage systems, in CSEE Journal of Power and Energy Systems, p 1-15.

[17] Li, S., and Ke, B., 2011. Study of battery modeling using mathematical and circuit oriented approaches, 2011 IEEE Power and Energy Society General Meeting. pp. 1-8.

[18] Baronti, F., Di Rienzo, R., Papazafiropulos, N., Roncella, R. and Saletti, R., 2014. Investigation of series-parallel connections of multi-module batteries for electrified vehicles, 2014 IEEE International Electric Vehicle Conference (IEVC), 17-19 Dec, Florence, Italy, pp. 1-7.

[19] Enache, B., Alexandru, M. E., and . Constantinescu, L., 2015. Extending the battery model from a single cell to a battery pack with BMS, 2015 7th International Conference on Electronics, Computers and Artificial Intelligence (ECAI), 25-27 June, Bucharest, Romania, pp. AE-5-AE-14.

[20] Kim, J., Cho, B.H., 2013. Screening process-based modeling of the multi-cell battery string in series and parallel connections for high accuracy state-of-charge estimation, Energy, Volume 57, Pages 581-599.

[21] Zhang, Y., and Lu, S., 2018. Research on Series-Parallel Connection Switching Charging Method for Lithium Battery of Autonomous Underwater Vehicles, 2018 IEEE 8th International Conference on Underwater System Technology: Theory and Applications (USYS), 1-3 Dec, Wuhan, China, pp. 1-5.

[22] Sen, C., and Kar, N. C., 2009. Battery pack modeling for the analysis of battery management system of a hybrid electric vehicle, 2009 IEEE Vehicle Power and

Propulsion Conference, 7-10 Sept, Dearborn, MI, USA, pp. 207-212.

[23] Lawder, M. T., et al. 2014. Battery Energy Storage System (BESS) and Battery Management System (BMS) for Grid-Scale Applications," in Proceedings of the IEEE, vol. 102, no. 6, pp. 1014-1030.

[24] Capizzi, G., Bonanno, F., and Napoli, C., 2011. Recurrent neural network-based control strategy for battery energy storage in generation systems with intermittent renewable energy sources, 2011 International Conference on Clean Electrical Power (ICCEP), 14-16 June, Ischia, Italy, pp. 336-340.

[25] Montoya Giraldo, O. D., Gil González, W. J., Garcés Ruiz, A., Escobar Mejía, A., and Grisales Noreña, L. F., 2018. Nonlinear Control for Battery Energy Storage Systems in Power Grids, 2018 IEEE Green Technologies Conference (GreenTech), 4-6 April, Austin, TX, USA, pp. 65-70.

[26] Giannoutsos, S. V., and Manias, S. N., 2012. A cascade control scheme for a grid connected Battery Energy Storage System (BESS), 2012 IEEE International Energy Conference and Exhibition (ENERGYCON), 9-12 Sept, Florence, Italy, pp 469-474.

[27] Levron, Y., and Belikov, J., (2017). Modeling power networks using dynamic phasors in the dq0 reference frame, Electric Power Systems Research, Volume 144, Pages 233-242.

[28] De Breucker, Engelen, S., K., D'hulst, R. and Driesen, J., 2013. Impact of current ripple on Li-ion battery ageing, 2013 World Electric Vehicle Symposium and Exhibition (EVS27), 17-20 Nov, Barcelona, Spain, pp. 1-9.